Electron paramagnetic resonance properties of Gd^{3+} ions in $PbWO_4$ scintillator crystals

2006 J. Phys.: Condens. Matter 18 719

(http://iopscience.iop.org/0953-8984/18/2/025)

INSTITUTE OF PHYSICS PUBLISHING JOURNAL OF PHYSICS: CONDENSED MATTER

J. Phys.: Condens. Matter **18** (2006) 719–728 doi:10.1088/0953-8984/18/2/025

Electron paramagnetic resonance properties of Gd^{3+} ions in $PbWO_4$ scintillator crystals

S V Nistor[1], M Stefan[1,4], E Goovaerts[2], M Nikl[3] and P Bohacek[3]

[1] National Institute for Materials Physics, POB MG-7, Magurele, Bucharest, RO-077125, Romania
[2] Department of Physics, University of Antwerp, Campus Drie Eiken, Universiteitsplein 1, BE-2610 Antwerp, Belgium
[3] Institute of Physics AS CR, Cukrovarnicka 10, 16200 Prague 6, Czech Republic

E-mail: mstefan@infim.ro

Received 3 November 2005
Published 16 December 2005
Online at stacks.iop.org/JPhysCM/18/719

Abstract

The properties of the electron paramagnetic resonance spectra of Gd^{3+} ions in $PbWO_4$ single crystals have been investigated in the X-band microwave frequency region, in the 1.5 to 290 K temperature range. The observed S_4 symmetry of the local crystal field at the Gd^{3+} impurity ions strongly suggests that the Gd^{3+} ions substitute for the Pb^{2+} lattice cations, with charge compensation at a distance. The spin Hamiltonian parameters are comparable with those of the Gd^{3+} ions in other isomorphous tungstates. The temperature variation of the fine structure parameters B_2^0 and B_4^0 points to an energy transfer between the impurity ions and the host lattice, which takes place mainly through a local vibrational mode of frequency $\omega = 3.1 \times 10^{13}$ rad s^{-1}.

1. Introduction

Scintillating $PbWO_4$ (PWO) with scheelite structure has been the subject of intense scrutiny during the past decade, due to its approved applications in large scale projects in high energy and nuclear physics (for a review see [1]). After the initial optimization of its radiation resistance and speed of scintillation response, new ways of increasing the light yield have been searched for. It is thus worth mentioning the double doping with Mo, A^{3+} (A = Y, La) [2, 3], the annealing treatments [4], and the recent double doping with La and Y, which proved successful in applications where the crystals were cooled below room temperature [5]. The latter approach can be understood in the light of the increased stability of defect-perturbed (localized) exciton states, which shape the temperature dependence of the emission intensity above 200 K in PWO [6, 7]. Increased scintillation efficiency of PWO might open the way towards new applications in the field of medical imaging, radiation defectoscopy, safety, etc.

[4] Author to whom any correspondence should be addressed.

Aliovalent impurity ions present in the PWO crystal lattice influence the energy balance in the crystal and affect the scintillation properties and the energy transfer, and the storage processes in general. By a corresponding choice of doping it is possible to improve the performances for specific applications. Similarly to other selected trivalent ions [1], Gd^{3+} was found to induce faster scintillation and photoluminescence response, to suppress the deep trap states and to improve the radiation resistance and transmission in the 350–500 nm range [8]. The mechanisms underlying these effects are not completely understood, but the interaction between the impurity ion and the host lattice is expected to play an important role.

In this work we report the results of electron paramagnetic resonance (EPR) investigations, in the 1.5–290 K temperature range, on PWO single crystals containing low concentrations (<1 ppm) of Gd^{3+} ions. We were able to determine the localization of these ions in the crystal lattice, the properties of their spin ground state, as well as the mechanism of the spin–lattice coupling and the characteristics of the local crystalline field.

2. Experimental details

Our studies were carried out on the same PWO single-crystalline samples as were previously used in EPR investigations of the Mn^{2+} impurity ions [9, 10]. The single crystals were grown by the Czochralski method in air, with the seed parallel to the *c* crystalline direction, from 5N purity powders. The undoped, as well as the Sn (300 ppm) and Bi (600 ppm) doped single crystals showed similar Mn^{2+} and Gd^{3+} spectra, attributed to unintended impurities with very low concentrations (<1 ppm), and thus we used EPR samples conveniently cut from these crystals. The samples, $2.5 \times 2.5 \times 10$ mm^3 in size, were x-ray oriented and cut with the long/rotation axis along one of the *a*, ⟨110⟩ or *c* crystal axes with an accuracy of $\pm 1^\circ$. The crystal axes could be further oriented parallel to the rotation axis of the electromagnet with an estimated accuracy better than $\pm 0.1^\circ$ by tilting the sample cavity with respect to the magnetic field rotation axis.

The EPR measurements were carried out on a Bruker ESP 300E X-band spectrometer equipped with a gas-flow cryogenic system (ESR910 from Oxford Instruments), allowing operation from room temperature (RT) down to 1.5 K. Special care was taken in accurately measuring the sample temperature. Indeed, due to the relatively large diameter of the sample holder, which impeded the helium gas flow in the sample compartment, the temperature gradient at the sample position could be quite large. As we found out with a thermocouple inserted in a dummy sample, the temperature reading of the inset thermocouple (that was part of the temperature control unit and fixed at about 1 cm below the sample) could be up to 10 K different from the real temperature at the sample position. In order to determine more accurately the sample temperature, in past measurements on the Mn^{2+} ions [10] we employed a specially built sample holder, equipped with a second thermocouple that read the temperature a few millimetres above the top of the sample. In those measurements the sample temperature was determined as the average of the readings made with the controller thermocouple and holder thermocouple, respectively, measurements made in conditions of reduced temperature gradients (large helium flows). The past measurements on Mn^{2+} impurity ions, which were simultaneously present in the crystals studied, provided us with a temperature etalon as well, namely the temperature dependence of the extension of the whole Mn^{2+} EPR spectrum, as discussed in [10]. We could thus use this ad hoc Mn^{2+} based thermometer for temperature determination with an accuracy of $\pm$ 1 K.

The numerical analysis of the investigated EPR spectra was performed with the EPRNMR (version 6.5) [11] and SIM [12, 13] computer programs.

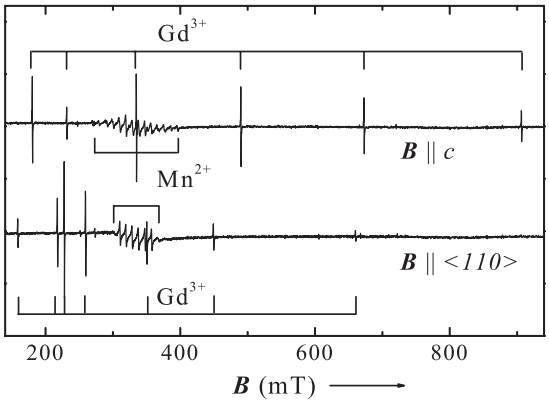

Figure 1. The EPR spectra of the Gd^{3+} ions in the PWO crystals recorded in the X-band for the $\boldsymbol{B} \parallel c$ and $\boldsymbol{B} \parallel \langle 110 \rangle$ orientations, respectively, at room temperature (RT).

3. EPR parameters of Gd^{3+} ions in PWO

The scheelite-type PWO crystals (space group $I4_1/a$, $a = 5.456$ Å, $c = 12.020$ Å) are characterized by a square lattice of identical columns of Pb and W atoms parallel to the z axis, each column being made by a regular stacking of Pb and W atoms [14]. The W^{6+} ions are located at the centre of isolated regular O^{2-} tetrahedra, with bond length $R(W-O) = 1.795$ Å. The Pb^{2+} ions are inside a distorted dodecahedron of O^{2-} belonging to eight different WO_4^{2-} units, resulting in S_4 site symmetry.

The EPR spectra of Gd^{3+} consist of several fine structure ($\Delta M_S = \pm 1, \pm 2$) narrow lines (0.17 mT peak-to-peak linewidth at RT for the $-1/2 \leftrightarrow 1/2$ transition), which are strongly saturated at low temperatures (see figure 1). Each line has two sets of four satellite lines which are fully resolved at $T < 200$ K, whose intensity and separation correspond to the ^{155}Gd and ^{157}Gd isotopes (14.80% and 15.65% abundance, respectively), both with nuclear spin $I = 3/2$ and magnetic moments $^{155}\mu = -0.2591\mu_n$ and $^{157}\mu = -0.3399\mu_n$, respectively (see figure 2).

We have determined the angular dependence of the EPR spectra at 26 K and RT, in the (ab) and (110) crystallographic planes (see figures 3(a) and (b)). In order to obtain a high precision in the magnetic field values (±0.02 mT), the Gd^{3+} EPR lines were recorded individually, with a field sweep of 2–5 mT (for large field sweeps, >500 mT, the digitally read magnetic field deviates non-linearly from the actual field values, depending on the field sweep and the time constant values involved).

The crystals were accurately oriented in the resonance cavity with the magnetic field parallel to the c crystalline direction, using the strong (ac) angular dependence of the Gd^{3+} spectra. The Mn^{2+} spectra were also used for orientation, due to the fact that the whole Mn^{2+} spectrum has the largest extension along the c direction and the highest line amplitude (smallest linewidth) of the non-central transitions along the a and c directions [10].

The EPR spectra of the Gd^{3+} ions are described with a typical spin Hamiltonian (SH) for an axial centre, expressed in the Oabc reference crystal axes, with $S = 7/2$ and $I = 3/2$ for the two odd isotopes [15]:

$$H = \mu_B S \cdot g \cdot \boldsymbol{B} + B_2^0 \cdot O_2^0 + B_4^0 \cdot O_4^0 + B_4^4 \cdot O_4^4 + B_4^{-4} \cdot O_4^{-4} + B_6^0 \cdot O_6^0 + B_6^4 \cdot O_6^4 + B_6^{-4} \cdot O_6^{-4} + S \cdot \boldsymbol{A} \cdot I - g_n \mu_n \boldsymbol{B} \cdot I. \quad (1)$$

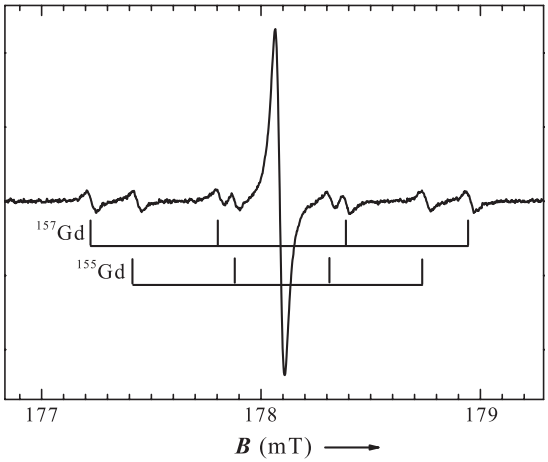

Figure 2. The EPR fine structure (M_S: $-3/2 \leftrightarrow -1/2$) transition of the Gd^{3+} ions in the PWO crystals, for $\boldsymbol{B} \parallel c$ and $T = 100$ K, exhibiting the resolved hyperfine structure from the two odd ^{155}Gd and ^{157}Gd isotopes.

Table 1. The spin Hamiltonian (SH) parameters of the Gd^{3+} ions in $PbWO_4$ at 26 K and RT (this work) in comparison with similar data for PWO at RT [16]. The spin Hamiltonian is expressed in the crystallographic axes reference system O*abc*.

	Temperature		
EPR parameters	$T = 26$ K	$T = 293$ K	RT [16]
$g_\perp$	1.9913 ± 0.0005	1.9916 ± 0.0005	1.9922
$g_\parallel$	1.9916 ± 0.0005	1.9918 ± 0.0005	1.9923
B_2^0 (MHz)	-852.3 ± 0.5	-821.1 ± 0.5	-820.2
B_4^0 (MHz)	-0.914 ± 0.005	-0.855 ± 0.005	-0.851
B_4^4 (MHz)	-4.91 ± 0.07	-4.65 ± 0.07	-6.615
B_4^{-4} (MHz)	-4.89 ± 0.07	-4.76 ± 0.07	
B_6^0 (MHz)	$(8.6 \pm 0.8) \times 10^{-4}$	$(9.0 \pm 0.8) \times 10^{-4}$	$\leqslant 2.38 \times 10^{-4}$
B_6^4 (MHz)	$(-5 \pm 2) \times 10^{-4}$	$(9 \pm 2) \times 10^{-4}$	0.0067
B_6^{-4} (MHz)	$(96 \pm 5) \times 10^{-4}$	$(85 \pm 5) \times 10^{-4}$	—
$^{155}A_\perp$ (MHz)	8.45 ± 0.15[a]		—
$^{155}A_\parallel$ (MHz)	12.21 ± 0.15[a]		—
$^{157}A_\perp$ (MHz)	11.18 ± 0.15[a]		—
$^{157}A_\parallel$ (MHz)	16.11 ± 0.15[a]		—

[a] The hyperfine splitting is constant within the experimental accuracy in the investigated temperature range.

As shown by the angular dependence of the EPR spectrum (see figures 3(a) and (b)), the local symmetry of the Gd^{3+} paramagnetic centre is tetragonal (S_4), with the z axis parallel to the c crystalline axis and the x axis rotated from the a crystalline direction at an angle of 11.2°. The complete sets of EPR parameters, determined at two different temperatures, 26 K and RT, are reported in table 1. They have been obtained by numerical simulation of the EPR line positions with the spin Hamiltonian (1) and fitting with experimental data measured in the two crystallographic planes (ab) and (110) by rotation in steps of 5°.

Table 1 also presents the fine structure EPR parameters of the Gd^{3+} ions in PWO, which have been previously determined by Meilman [16] only at RT, in the O*abc* coordinate system. There are small differences between the parameter values reported by us and those of Meilman,

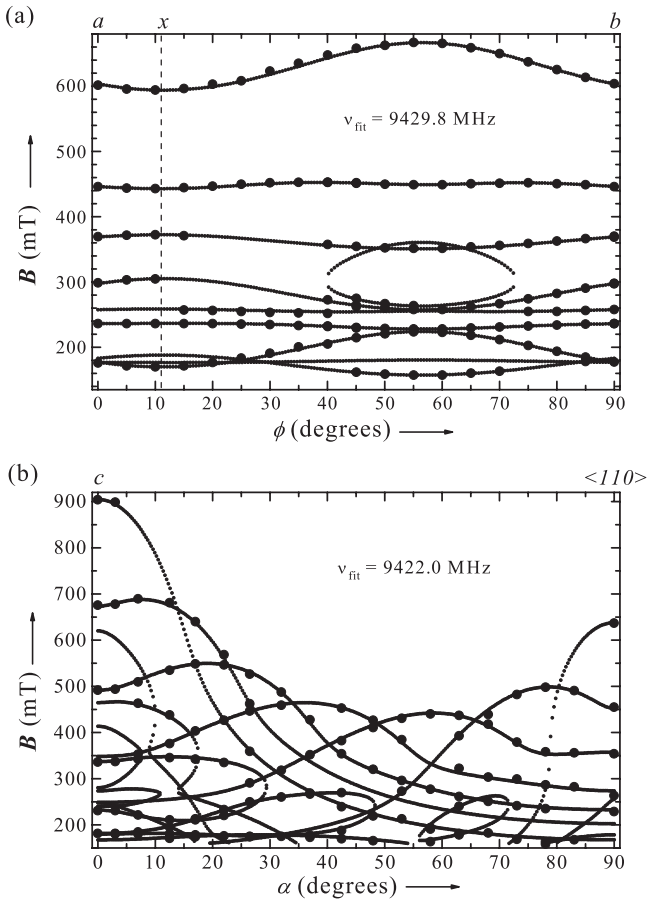

Figure 3. Experimental (solid circles) and calculated (dotted lines) angular dependence of the fine structure EPR lines of Gd^{3+} ions in the PWO crystals, for: (a) $\boldsymbol{B}$ in the (ab) plane, and (b) $\boldsymbol{B}$ in the (110) plane, at $T = 293$ K. The size of the experimental points accounts for the experimental error in the reading of both magnetic field and angle value.

due to the fact that he used a simpler approach, by taking the EPR tensor axes aligned with the crystalline axes and neglecting the $B_l^{-m}\boldsymbol{O}_l^{-m}$ terms, which should also be considered for an S_4 site symmetry [17]. One should also mention that the hyperfine parameters obtained by us are very close to the hyperfine parameters of Gd^{3+} in $CaWO_4$ along the c direction determined by Hempstead and Bowers at 77 K: $^{155}A_{\parallel} = 12.47$ MHz and $^{155}A_{\parallel} = 16.37$ MHz [18].

As shown in table 2, the EPR parameters of Gd^{3+} ions in PWO are comparable with those of the Gd^{3+} ions in other crystals from the scheelite series [19]. This observation has allowed us to attribute a negative value to the largest zero-field-splitting (ZFS) parameter B_2^0, which determines the sign of the other ZFS parameters B_l^{-m}. Any attempts to determine experimentally the sign of B_2^0, by observing the relative intensity of the various fine structure lines at low measuring temperatures, have failed because of the strong saturation effects, even for the lowest attainable microwave power.

4. The temperature dependence of the Gd^{3+} EPR parameters in PWO

We have also studied the temperature dependence of the EPR parameters for the Gd^{3+} ions in PWO. The temperature dependence measurements were carried out for the magnetic field

Table 2. ZFS parameters of Gd^{3+} in PWO (present work) and other scheelite-type compounds [19] at RT. The reference system used in [19] was the O*abc* crystallographic system.

Host lattice	B_2^0 (MHz)	B_4^0 (MHz)	B_6^0 (MHz)	B_4^4 (MHz)	B_6^4 (MHz)
$CaWO_4$	−893.3	−1.14	6.0×10^{-4}	−7.02	4.8×10^{-4}
$SrWO_4$	−867.4	−0.85	0	−5.95	0
$PbWO_4$[a]	−821.1	−0.85	9.0×10^{-4}	−6.61	38×10^{-4}
$BaWO_4$	−872.4	−0.65	0	−5.65	0
$CaMoO_4$	−854.6	−0.84	$\leqslant 0.7 \times 10^{-4}$	−4.61	76×10^{-4}
$SrMoO_4$	−806.6	−0.65	0	−3.35	0
$PbMoO_4$	−799.5	−0.60	0	−4.55	0

[a] Present work; for the sake of comparison we have written the parameters in the local O*xyz* reference system, with $z \parallel c$ and x in the (ab) plane at 11.2° from a, where $B_l^{-4} = 0$.

along the c and a main crystalline directions, where c was parallel to the main z direction of the EPR tensors. For each measuring temperature we also recorded the Mn^{2+} spectrum, in order to determine the real temperature of the sample from this spectrum extension. Because very few EPR transitions were visible in each direction, a complete set of the EPR parameters could not be determined from fitting the spectra recorded only along these two directions. However, the spectra angular dependences measured at 26 K and RT, respectively, provided sets of EPR parameter values that allowed us to make several assumptions in order to further simplify the procedures. As one can see from table 1, there are several parameters, namely g and B_6^m, where $m = 0, 4, -4$, that exhibit a very small temperature variation in the 26–293 K range, comparable to the measuring error. Moreover, the hyperfine parameters were practically constant within the limits of experimental errors. Consequently, we used, during the fitting procedure for each measuring temperature, either the values obtained by a linear interpolation of the extreme values, or constant values in the case of the hyperfine parameters. Throughout the fitting procedures the parameters were written in the local O*xyz* reference system, with $z \parallel c$ and x in the (ab) plane at 11.2° from a. This procedure has the advantage that $B_l^{-4} = 0$, where $l = 4, 6$.

As shown in figures 4 and 5, the absolute values of the B_2^0 and B_4^0 parameters exhibit a monotonous decrease with temperature.

The thermal expansion was shown to have negligible influence on the EPR parameters of Mn^{2+} in PWO and other crystals from the scheelite family [20] and of Gd^{3+} in $CaWO_4$ [21]. In both cases this conclusion was drawn based on similarities of temperature behaviour of each impurity ion in several host crystals. Thus, we are further considering that the thermal expansion plays a negligible role in the temperature variation of the Gd^{3+} ZFS parameters in PWO as well, the main contribution being due to the explicit effects [20, 22].

We found out that for both B_2^0 and B_4^0 parameters the temperature variation could be very well fitted considering the influence of a local vibration mode [22, 23]:

$$|B_1^0|(T) = \beta_0 + \beta_1 \coth(\hbar\omega/2k_B T). \tag{2}$$

Here the first term is the static parameter value and the second term describes the coupling of the Gd^{3+} ion with a resonant mode of frequency ω.

The fitting parameters were found to be: $\beta_0 = -870.6 \pm 1.4$ MHz, $\beta_1 = 18.7 \pm 1.5$ MHz and $\omega = (3.1 \pm 0.2) \times 10^{13}$ rad s^{-1} for B_2^0, and $\beta_0 = -0.953 \pm 0.003$ MHz, $\beta_1 = 0.039 \pm 0.003$ MHz and $\omega = (3.2 \pm 0.2) \times 10^{13}$ rad s^{-1} for B_4^0. The resulting fitting curves are represented with dotted lines in figures 4 and 5, respectively. These results show that the local vibrational mode is strong enough to be practically responsible for the coupling of the spin of the gadolinium ions with the crystal lattice [24]. The presence of such a mode could

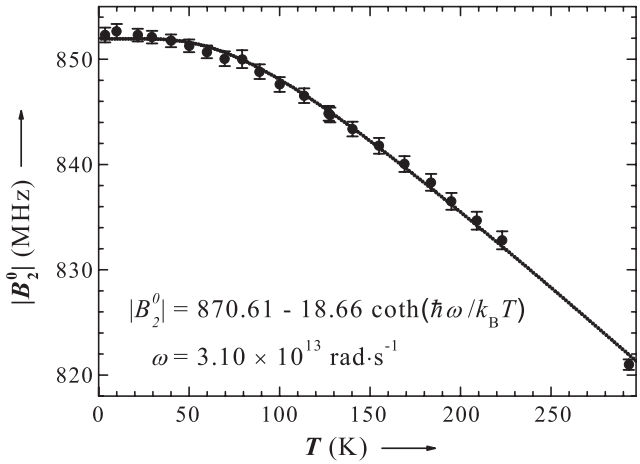

Figure 4. The temperature variation of the absolute value of the B_2^0 parameter for the Gd^{3+} ions in the PWO crystals. Solid circles: experimental data. Dotted line: calculated temperature dependence.

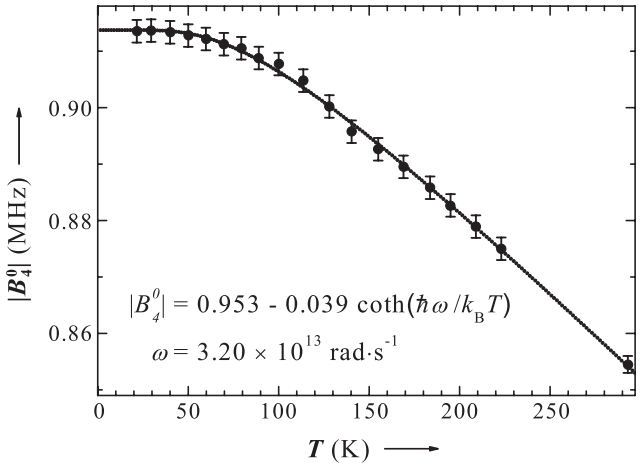

Figure 5. The temperature variation of the absolute value of the B_4^0 parameter for the Gd^{3+} ions in the PWO crystals. Solid circles: experimental data. Dotted line: calculated temperature dependence.

be explained [25] by the mass difference between the Gd^{3+} and Pb^{2+} ions, which is about 24%. The presence of a local vibrational mode has been also used to explain the temperature dependence of the EPR parameters of Mn^{2+} in PWO [10]. However, in that case the frequency of the local mode was found to be 3.5 times smaller compared to the case of Gd^{3+}, although the mass difference between Mn^{2+} and Pb^{2+} ions is larger (73%). One could explain the observed stronger local coupling in the case of the Gd^{3+} ions by the stiffening of the unit cell induced by the Coulombic forces due to the locally uncompensated extra positive charge of the impurity ion [21].

The temperature variation of the absolute value of the B_4^4 parameter exhibits a clear decrease in the temperature range investigated. However, as shown in figure 6, its variation between adjacent experimental measuring points is comparable with the experimental error.

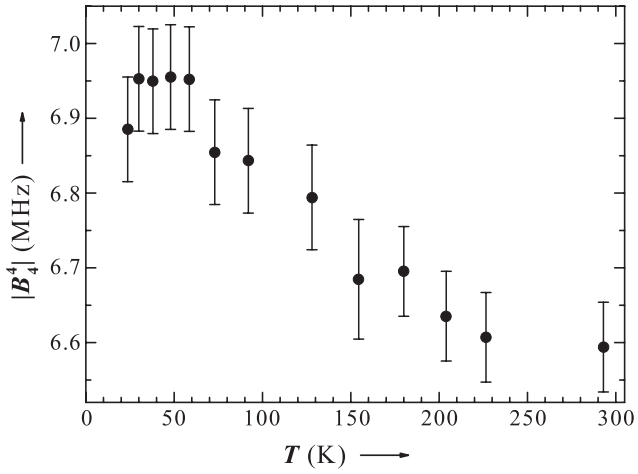

Figure 6. The temperature variation of the absolute values of the B_4^4 parameter for the Gd^{3+} ions in the PWO crystals, given in the local $Oxyz$ reference axes system.

For this reason it has been impossible to describe it univocally with a definite functional dependence.

5. Discussion and conclusions

The analysis of the EPR spectra of the Gd^{3+} ions in PWO single crystals shows a S_4 tetragonal symmetry of the local crystal field with EPR parameter values comparable to those determined for other crystal lattice hosts of the scheelite family. Thus, one could assume that the Gd^{3+} ions substitute for the Pb^{2+} lattice cations in PWO, as they do in the other scheelites. This conclusion is further supported by the analysis of the B_2^0 parameter using the superposition model [26]. According to this model, the ZFS parameters of a paramagnetic ion can be expressed as linear combinations of separate contributions from the neighbouring ligands:

$$b_k^q = \sum_i \bar{b}_k(R_i) K_k^q(\theta_i, \varphi_i). \tag{3}$$

Here K_k^q is a coordination factor determined by the angular position of the ligand i and $\bar{b}_k(R_i)$ is the 'intrinsic' parameter specific for each type of paramagnetic ion–ligand chemical bond and depending on the distance only. Within a group of isomorphous host crystals in which the interionic distances do not vary much, the radial dependence of the 'intrinsic' parameter can be expressed as

$$\bar{b}_k(R) = \bar{b}_k(R_0)\left(\frac{R_0}{R}\right)^{t_k}. \tag{4}$$

Here R_0 is an average distance and t_k is usually optimized for a certain configuration and type of ligands.

In the scheelite-type crystals with formula AMO_4, where A = Pb, Ca, Sr, Ba and M = W, Mo, the eight nearest oxygen ligands are grouped into two sets of four, as regards their separation (bond lengths) from the central A^{2+} ion. In the case of PWO, the bond lengths are R_1(Pb–O) = 2.580 Å and R_2(Pb–O) = 2.637 Å at room temperature [14]. In the Oabc crystal axes reference system the directions of the Pb–O bonds are defined by the polar angles $\theta_1 = 38.52°$, $\phi_1 = 62.51°$ and $\theta_2 = 111.98°$, $\phi_2 = 54.34°$, respectively. The

corresponding coordination factors for the second-order ZFS parameter, calculated according to the superposition model for the two sets of oxygens, are $K_2^0(R_1) = -1.1594$ and $K_2^0(R_2) = 1.6727$.

Applying equations (3) and (4) to the case at hand, the second-order ZFS parameter can be expressed as

$$b_2^0 = \bar{b}_2(R_0)\left[K_2^0(1)(R_0/R_1)^{t_2} + K_2^0(2)(R_0/R_2)^{t_2}\right]. \tag{5}$$

Here $R_0 = 2.466$ Å, calculated as the average Gd^{3+}–O^{2-} distance in $CaMoO_4$, $t_2 = 2.5$ and $\bar{b}_2(R_0) = -5150.44$ MHz is the second-order intrinsic parameter [19].

With the coordination factors previously calculated one obtains $b_2^0 = -2647.3$ MHz, which is reasonably close to the experimental value $b_2^0 = 3B_2^0 = -2463.2$ MHz. We can conclude from the results of this analysis that the Gd^{3+} impurity ions do indeed substitute for the Pb^{2+} host ions in unperturbed S_4 tetragonal sites, the charge compensation of the positive extra charge of the impurity ion taking place at a distance.

The analysis of the temperature variation of the ZFS parameters of the Gd^{3+} ions in PWO crystals points to the presence of a single, resonant mode, which is due to the large mass difference between the substitutional Gd^{3+} impurity ions and the substituted Pb^{2+} host ions. The local vibrational mode at the Gd^{3+} impurity ions with a frequency $\omega = 3.1 \times 10^{13}$ rad s^{-1}, as determined from the temperature dependence of the B_2^0 and B_4^0 parameters, is dominating the spin–lattice interaction of the paramagnetic ion. Our results show that the energy transfer between the impurity ions and the host lattice takes place mainly through this vibrational mode, which is expected to further affect the luminescence properties of the PWO crystals doped with such impurities.

Acknowledgments

This work was performed in the framework of the bilateral scientific collaboration agreement between the National Institute for Materials Physics—laboratory 'Microstructure of Defects in Solids'—and the University of Antwerp—laboratory 'Experimental Condensed Matter Physics', with financial support from the Romanian Ministry of Education and Research (CERES project No 4-76/2004). Partial financial support by the Flemish Fund for Scientific Research (FWO), in the group project G.0409.02, and that of the Czech Institutional Research Plan AV0Z10100521 are also gratefully acknowledged.

References

[1] Nikl M 2000 *Phys. Status Solidi* a **178** 595
[2] Nikl M, Bohacek P, Vedda A, Martini M, Pazzi G P, Fabeni P and Kobayashi M 2000 *Phys. Status Solidi* a **182** R3
[3] Annenkov A, Borisevitch A, Hofstaetter A, Korzhik M, Ligun V, Lecoq P, Missevitch O, Novotny R and Peigneux J P 2000 *Nucl. Instrum. Methods* A **450** 71
[4] Kobayashi M, Usuki Y, Ishii I and Itoh M 2005 *Nucl. Instrum. Methods* A **537** 312
[5] Borisevich A, Fedorov A, Hofstaetter A, Korzhik M, Meyer B K, Missevitch O and Novotny R 2005 *Nucl. Instrum. Methods* A **537** 101
[6] Bohacek P, Fabeni P, Krasnikov A, Nikl M, Pazzi G P, Susini C and Zazubovich S 2005 *Radiat. Prot. Dosim.* doi:10.1093/rpd/nci580
[7] Krasnikov A, Nikl M and Zazubovich S 2005 Localized excitons and defects in $PbWO_4$ single crystals: the luminescence and photo-thermally stimulated disintegration study *Phys. Rev.* B submitted
[8] Baccaro S, Bohacek P, Cecilia A, Cemmi A, Croci S, Dafinei I, Diemoz M, Fabeni P, Ishii M, Kobayashi M, Martini M, Mihokova E, Montecchi M, Nikl M, Organtini G, Pazzi G P, Usuki Y and Vedda A 2000 *Phys. Status Solidi* a **179** 445

[9] Nistor S V, Stefan M, Goovaerts E, Nikl M and Bohacek P 2004 *Radiat. Meas.* **38** 655
[10] Stefan M, Nistor S V, Goovaerts E, Nikl M and Bohacek P 2005 *J. Phys.: Condens. Matter* **17** 719
[11] *Computer Program EPRNMR v. 6.5* (Canada: Department of Chemistry, University of Saskatchewan)
[12] Glerup J and Weihe H 1991 *Acta Chem. Scand.* **45** 444
[13] Jacobsen C J H, Pedersen E, Villadsen J and Weihe H 1993 *Inorg. Chem.* **32** 1216
[14] Moreau J M, Galez Ph, Peigneux J P and Korzhik M V 1996 *J. Alloys Compounds* **238** 46
[15] Abragam A and Bleaney B 1971 *Electron Paramagnetic Resonance of Transition Ions in Crystals* (Oxford: Clarendon)
[16] Meilman M L 1966 *Fiz. Tverd. Tela* **8** 3656
[17] McGavin D G 1987 *J. Magn. Reson.* **74** 19
[18] Hempstead C F and Bowers K D 1960 *Phys. Rev.* **118** 131
[19] Vishwamittar and Puri S P 1974 *J. Chem. Phys.* **61** 3720
[20] Biederbick R, Hofstaetter A and Scharmann A 1978 *Phys. Status Solidi* b **89** 449
[21] Harvey J S M and Kiefte H 1971 *Can. J. Phys.* **49** 996
[22] Walsh W M Jr, Jeener J and Bloembergen N 1965 *Phys. Rev.* **139** A1338
[23] Pfister G, Dreybrodt W and Assmus W 1969 *Phys. Status Solidi* **36** 351
[24] Bjork R L 1957 *Phys. Rev.* **105** 456
[25] Klemens P G 1962 *Phys. Rev.* **125** 1795
[26] Newman D J and Urban W 1975 *Adv. Phys.* **24** 793